

Fragmentation in $H \rightarrow b\bar{b}$ Processes

G. Corcella

Department of Physics, CERN
Theory Division
CH-1211 Geneva 23, Switzerland

Abstract

I study bottom quark fragmentation in the Standard Model Higgs decay $H \rightarrow b\bar{b}$, within the framework of perturbative fragmentation functions. I resum large collinear logarithms $\ln(m_H^2/m_b^2)$ in the next-to-leading logarithmic (NLL) approximation, using the DGLAP evolution equations. Soft contributions to the $\overline{\text{MS}}$ coefficient function and to the initial condition of the perturbative fragmentation function are resummed to NLL accuracy as well. The implementation of collinear and soft resummation has a relevant impact on the b energy spectrum, which exhibits a milder dependence on factorization and renormalization scales and on the Higgs mass. I present some predictions on the energy distribution of b -flavoured hadrons in Higgs decay, making use of data from LEP and SLD experiments to fit a few hadronization models. I also compare the phenomenological results yielded by a few processes recently provided with NLL collinear and soft resummations.

1 Introduction

The Higgs boson plays a crucial role in the Standard Model (SM) of electroweak interactions as it is responsible for the mechanism of mass generation. However, this particle has not yet been experimentally discovered.

Searches for the Standard Model Higgs boson have been performed at the LEP collider, are currently under way at the Tevatron, and will be ultimately one of the main goals of experiments at the LHC. (see, for a review, e.g. [1]). In detail, the LEP experiments have set a lower bound on the Higgs mass at $m_H > 114.4$ GeV [2], mainly using the production channel $e^+e^- \rightarrow HZ$. The Tevatron will be able to exclude a Higgs boson with mass lower than 130 GeV within three standard deviations [3]. Future experiments at the LHC will be capable of going beyond and exploring the Higgs mass spectrum from 100 GeV to about 1 TeV [4].

In order to accurately perform such searches, the use of precise QCD calculations will be fundamental. In this paper, I consider the decay of the Standard Model Higgs boson into $b\bar{b}$ pairs, i.e. $H \rightarrow b\bar{b}$. In fact, the favourite discovery channel of the Higgs at the Tevatron consists of processes where H is produced in association with a vector boson, i.e. $p\bar{p} \rightarrow VH$, where V is a Z or a W , followed by the decays $H \rightarrow b\bar{b}$ and $V \rightarrow \ell_1\ell_2$, ℓ_1 and ℓ_2 being leptons. At the LHC, the process $gg(q\bar{q}) \rightarrow H \rightarrow b\bar{b}$ will be affected by large QCD backgrounds, which make the detection of this decay channel more cumbersome. However, the process $H \rightarrow b\bar{b}$ will still play a role, in particular for $m_H \lesssim 135$ GeV and Higgs production in association with $t\bar{t}$ pairs, i.e. $p\bar{p} \rightarrow t\bar{t}H$ [5], with a W boson [6], in vector boson fusion [7].

Hereafter, I shall address the issue of multiple gluon radiation in $H \rightarrow b\bar{b}$ processes. While fixed-order calculations are reliable enough to predict total cross sections or widths, differential distributions present terms, corresponding to collinear- or soft-parton radiation, that need to be summed to all orders to obtain a reliable result.

In particular, large mass logarithms $\ln(m_H^2/m_b^2)$, which appear in the b -quark energy spectrum, can be resummed using the approach of perturbative fragmentation functions [8], which expresses the energy spectrum of a heavy quark as the convolution of a coefficient function, describing the emission of a massless parton, and a perturbative fragmentation function $D(m_b, \mu_F)$, associated with the fragmentation of a massless parton into a massive quark. The method of perturbative fragmentation can be used as long as the heavy-quark mass m is much smaller than the hard scale of the process Q , i.e. $m \ll Q$. Given the current limits on the Higgs mass [2], the perturbative fragmentation approach can certainly be used in $H \rightarrow b\bar{b}$, since $m_b \ll m_H$.

The dependence of $D(m_b, \mu_F)$ on the factorization scale μ_F is determined by solving

the Dokshitzer–Gribov–Altarelli–Parisi (DGLAP) evolution equations [9, 10], once an initial condition at a scale μ_{0F} is given. The universality of the initial condition of the perturbative fragmentation function, first computed in [8], has been proved in a more general way in [11].

Moreover, both coefficient function and initial condition of the perturbative fragmentation function contain terms that become large once the b energy fraction x_b gets close to 1. Such terms correspond to soft-gluon emission, and need to be resummed. These contributions are process-dependent in the coefficient function and process-independent in the initial condition of the perturbative fragmentation function. The resummation of soft contributions to the coefficient function of $H \rightarrow b\bar{b}$ will be investigated below.

Finally, in order to describe the b -quark non-perturbative fragmentation into b -flavoured mesons or baryons B , some phenomenological hadronization models can be used. Relying on the universality of the hadronization mechanism, we can tune such models to data on B production in e^+e^- annihilation data from LEP or SLD and use them to predict the B -hadron spectrum in Higgs decay. Alternatively, we can use experimental data on the moments of the B spectrum in e^+e^- processes, fit the moments of the non-perturbative fragmentation function and predict hadron-level moments in Higgs decay.

The plan of this paper is the following. In Section 2, I describe the calculation of the next-to-leading order (NLO) $\overline{\text{MS}}$ coefficient function. The approach of perturbative fragmentation and the resummation of collinear logarithms $\ln(m_H^2/m_b^2)$ will be discussed in Section 3. Section 4 describes the implementation of soft resummation in the coefficient function. In Section 5, I shall present results on the b -quark energy spectrum in top decay and investigate the effect of soft and collinear resummation. In Section 6, hadron-level results in x_B and N spaces are presented, while Section 7 summarizes the main results and gives some concluding remarks.

2 NLO coefficient function

I consider Higgs decay into $b\bar{b}$ pairs at next-to-leading order (NLO) in the strong coupling constant α_S

$$H(p_H) \rightarrow b(p_b)\bar{b}(p_{\bar{b}})(g(p_g)), \quad (1)$$

and define the variables:

$$x_b = \frac{2p_b \cdot p_H}{m_H^2}, \quad x_g = \frac{2p_g \cdot p_H}{m_H^2}. \quad (2)$$

The quantities x_b and x_g are the normalized energy fractions of b and g in the Higgs rest frame. As they are expressed in the form of Lorentz-invariant quantities, they can

be computed in any frame, provided that the four components of the momenta of b , g and H are known.

In the framework of perturbative fragmentation functions, since $m_b \ll m_H$, one can write the differential width for the production of a massive b quark in Higgs decay via the convolution:

$$\frac{1}{\Gamma_0} \frac{d\Gamma_b}{dx_b}(x_b, m_H, m_b) = \sum_i \int_{x_b}^1 \frac{dz}{z} \left[\frac{1}{\Gamma_0} \frac{d\hat{\Gamma}_i}{dz}(z, m_H, \mu, \mu_F) \right]^{\overline{\text{MS}}} D_i^{\overline{\text{MS}}} \left(\frac{x_b}{z}, \mu_F, m_b \right) + \mathcal{O}((m_b/m_H)^p) . \quad (3)$$

In Eq. (3), $d\hat{\Gamma}_i/dz$ is the differential width for the production of a massless parton i in Higgs decay with an energy fraction z , $D_i(x, \mu_F, m_b)$ is the perturbative fragmentation function for a parton i to fragment into a massive b quark, μ and μ_F are the renormalization and factorization scales, Γ_0 is the width of the Born process $H \rightarrow b\bar{b}$. The term $\mathcal{O}((m_b/m_H)^p)$, with $p \geq 1$, represents contributions which are power-suppressed for $m_b \ll m_H$.

In this section I discuss the computation of the coefficient function $(1/\Gamma_0)d\hat{\Gamma}_i/dz$, for the production of a massless b in the $\overline{\text{MS}}$ factorization scheme. I shall neglect secondary $b\bar{b}$ production from gluon splitting and limit myself to considering the perturbative fragmentation of a massless b into a massive b . In the summation on the right-hand side of Eq. (3) I shall have only the $i = b$ contribution.

I regularize ultraviolet, soft and collinear singularities in dimensional regularization, and define the parameter ϵ , which is related to the number of dimensions d via $d = 4 - 2\epsilon$. In the computation of $d\hat{\Gamma}_b/dz$, care is to be taken about the treatment of the Yukawa coupling of the $Hb\bar{b}$ vertex. In fact, if the bare Yukawa coupling y_b were used, the result would be the following:

$$\begin{aligned} \frac{d\hat{\Gamma}_b^{(0)}}{dz}(z, m_H, \mu, \mu_r) &= \Gamma_0 \left\{ \delta(1-z) + \frac{\alpha_S(\mu)}{2\pi} \left[P_{qq}(z) - 3C_F\delta(1-z) \right] \right. \\ &\quad \times \left. \left(-\frac{1}{\epsilon} + \gamma_E + \ln \frac{m_H^2}{4\pi\mu_r^2} \right) + G(z) \right\} . \end{aligned} \quad (4)$$

In Eq. (4), μ_r is the regularization scale, remnant of the regularization procedure, $G(z)$ is a function, independent of ϵ and μ_r , whose expression will be detailed later, $\gamma_E = 0.577 \dots$ is the Euler constant, $C_F = 4/3$, $P_{qq}(z)$ is the Altarelli–Parisi splitting function:

$$P_{qq}(z) = C_F \left(\frac{1+z^2}{1-z} \right)_+ . \quad (5)$$

Also, in Eq. (4) I have factorized the four-dimension Born width:¹

$$\Gamma_0 = \frac{3}{16\pi} m_H y_b^2. \quad (6)$$

Equation (4) shows that a pole $1/\epsilon$ is still present in the differential width. The contribution proportional to $P_{qq}(z)$ is associated with collinear radiation from the massless b quark and needs to be subtracted to give the coefficient function. Analogous contributions have been found, e.g. in the computation of the differential rate of other processes such as e^+e^- annihilation [8] or top decay [12]. The additional term, where the pole $1/\epsilon$ multiplies the quantity $\sim 3\alpha_S C_F \delta(1-z)$, instead has ultraviolet origin, and is characteristic of Higgs decay and of the scalar nature of the coupling of the Higgs to quarks. In fact, unlike the vectorial current, which is conserved, the scalar current is anomalous. Because of this extra term, if one naively calculated the total width integrating Eq. (4), one would still find the $1/\epsilon$ pole, which is clearly unphysical.²

In order to get a physical result, one must renormalize the Yukawa coupling. In the $\overline{\text{MS}}$ renormalization scheme, the renormalized coupling $\bar{y}_b(\mu)$ is related to y_b via (see, for instance, the discussion in Appendix D of Ref. [13]):

$$\bar{y}_b(\mu) = y_b \left\{ 1 - \frac{\alpha_S(\mu) C_F}{4\pi} \left[4 + 3 \left(-\frac{1}{\epsilon} + \gamma_E + \log \frac{m_H^2}{4\pi\mu^2} \right) \right] + \mathcal{O}(\alpha_S^2) \right\}. \quad (7)$$

One can therefore reabsorb the term $\sim 3\alpha_S C_F \delta(1-z)$ of Eq. (4) in the $\overline{\text{MS}}$ -renormalized coupling $\bar{y}_b(m_H)$ and evaluate the Born width in (6) in terms of $\bar{y}_b(m_H)$.

In the SM the Yukawa coupling is proportional to the quark mass and, as discussed in [13], Eq. (7) is consistent with expressing $\bar{y}_b(m_H)$ in terms of the $\overline{\text{MS}}$ b mass, $\bar{m}_b(m_H)$:

$$\bar{y}_b(m_H) = \frac{g \bar{m}_b(m_H)}{\sqrt{2} m_W}, \quad (8)$$

where m_W is the W mass and g is the coupling constant of $SU(2)$.

Furthermore, in Refs. [14, 15], where the authors performed the computation with a massive b quark, it was shown that a large logarithm $\sim \alpha_S \ln(m_H^2/m_b^2)$ appears in the NLO total rate if one uses the b -quark pole mass in the coupling. Such a mass logarithm can be reabsorbed in the $\overline{\text{MS}}$ mass $\bar{m}_b(m_H)$, which is related to the pole mass m_b by:

$$\bar{m}_b(m_H) = m_b \left[1 - \frac{\alpha_S(m_H) C_F}{4\pi} \left(4 + 3 \ln \frac{m_H^2}{m_b^2} \right) + \mathcal{O}(\alpha_S^2) \right]. \quad (9)$$

¹In order to get the correct finite term in Eq. (4), one should compute the LO width to $\mathcal{O}(\epsilon)$ in dimensional regularization. The d -dimension width Γ_d is related to Γ_0 by: $\Gamma_d = \Gamma_0 (4\pi/m_H^2)^\epsilon [1 + \epsilon(2 - \gamma)]$. Equations (4) and following account for the correct finite term.

² $P_{qq}(z)$ being an overall plus distribution, the integral of the term proportional to $P_{qq}(z)$ over z is clearly zero.

Subtracting the term $\sim P_{qq}(z)(-1/\epsilon + \gamma - \log 4\pi)$ from Eq. (4) and giving an explicit expression to the function $G(z)$, one will get the $\overline{\text{MS}}$ $H \rightarrow b\bar{b}$ coefficient function:

$$\begin{aligned} \left[\frac{1}{\bar{\Gamma}_0} \frac{d\hat{\Gamma}_b}{dz}(z, m_H, \mu, \mu_F) \right]^{\overline{\text{MS}}} &= \delta(1-z) + \frac{\alpha_S(\mu)C_F}{2\pi} \left[\left(\frac{1+z^2}{1-z} \right)_+ \ln \frac{m_H^2}{\mu_F^2} \right. \\ &+ \left(\frac{2}{3}\pi^2 + \frac{3}{2} \right) \delta(1-z) + 1-z - \frac{3}{2} \frac{z^2}{(1-z)_+} \\ &- (1+z)[\ln(1-z) + 2\ln z] + 6 \frac{\ln z}{(1-z)_+} \\ &\left. - 2 \frac{\ln z}{1-z} + 2 \left(\frac{\ln(1-z)}{1-z} \right)_+ \right]. \end{aligned} \quad (10)$$

In Eq. (10) I have accounted for the renormalization of the Yukawa coupling and denoted by $\bar{\Gamma}_0$ the LO width in terms of $\bar{y}_b(m_H)$. Also, in (10) the factorization scale μ_F will have to be taken of the order of the Higgs mass, in such a way that the logarithm $\ln(m_H^2/\mu_F^2)$ does not become too large.

In the following, I shall often make use of the $\overline{\text{MS}}$ coefficient function in Mellin moment space $\hat{\Gamma}_N$, which is defined by:

$$\hat{\Gamma}_N = \int_0^1 dz \, z^{N-1} \frac{1}{\bar{\Gamma}_0} \frac{d\hat{\Gamma}_b}{dz}(z). \quad (11)$$

In moment space Eq. (10) reads:

$$\begin{aligned} \hat{\Gamma}_N &= 1 + \frac{\alpha_S(\mu)C_F}{2\pi} \left\{ \left[\frac{1}{N(N+1)} - 2S_1(N) + \frac{3}{2} \right] \ln \frac{m_H^2}{\mu_F^2} \right. \\ &+ \frac{2}{3}\pi^2 + \frac{3}{2} + \frac{1}{N} - \frac{1}{N+1} + \frac{2}{N^2} + \frac{2}{(N+1)^2} \\ &- 4\psi_1(N) + \frac{1}{N}[\gamma + \psi_0(N+1)] + \frac{1}{N+1}[\gamma + \psi_0(N+2)] \\ &\left. + \frac{3}{2}S_1(N+1) + S_1^2(N-1) + S_2(N-1) \right\} \end{aligned} \quad (12)$$

In Eq. (12), I have introduced the polygamma functions, $\psi_k(x)$, which are related to the Euler gamma function $\Gamma(x)$ through:³

$$\psi_k(x) = \frac{d^{k+1} \log \Gamma(x)}{dx^{k+1}}. \quad (13)$$

³Reference [12] presents a typing mistake, since $\psi_k(x)$ is there defined as the k -th derivative of $\Gamma(x)$. The numerical results of [12] are nonetheless correct.

Equation (12) contains also the following combinations:

$$S_1(N) = \psi_0(N+1) - \psi_0(1), \quad (14)$$

$$S_2(N) = -\psi_1(N+1) + \psi_1(1). \quad (15)$$

In moment space the convolution (3) can then be rewritten as

$$\Gamma_N(m_H, m_b) = \hat{\Gamma}_N(m_H, \mu, \mu_F) D_{b,N}(\mu_F, m_b), \quad (16)$$

where $\Gamma_N(m_H, m_b)$ and $D_{b,N}(\mu_F, m_b)$ are the moments of the massive differential rate and of the perturbative fragmentation function, respectively.

3 Perturbative fragmentation and collinear resummation

The perturbative fragmentation function $D_b(x, \mu_F, m_b)$ introduced in Eq. (3) expresses the transition of a massless b into a massive b . Its value at any scale μ_F can be obtained by solving the DGLAP evolution equations [9, 10], once an initial condition is given. As shown in [11], as long as contributions proportional to powers of $(m_b/m_H)^p$ can be neglected, the initial condition of the perturbative fragmentation function at a scale μ_{0F} is process-independent. The NLO initial condition in the $\overline{\text{MS}}$ factorization scheme reads [8]:

$$D_b^{\text{ini}}(x_b, \mu_{0F}, m_b) = \delta(1 - x_b) + \frac{\alpha_S(\mu_0^2) C_F}{2\pi} \left[\frac{1 + x_b^2}{1 - x_b} \left(\ln \frac{\mu_{0F}^2}{m_b^2} - 2 \ln(1 - x_b) - 1 \right) \right]_+. \quad (17)$$

The authors of Ref. [16] have recently calculated $D_b^{\text{ini}}(x, \mu_{0F}, m_b)$ to next-to-next-to-leading order (NNLO), i.e. up to $\mathcal{O}(\alpha_S^2)$. For the purpose of this paper, where the coefficient function has been calculated to NLO, the perturbative fragmentation will be used to NLO as well.

The solution of the DGLAP equations in the non-singlet sector, for the evolution from the scale μ_{0F} to μ_F , is given by:

$$\begin{aligned} D_{b,N}(\mu_F, m_b) &= D_{b,N}^{\text{ini}}(\mu_{0F}, m_b) \exp \left\{ \frac{P_N^{(0)}}{2\pi b_0} \ln \frac{\alpha_S(\mu_{0F}^2)}{\alpha_S(\mu_F^2)} \right. \\ &\quad \left. + \frac{\alpha_S(\mu_{0F}^2) - \alpha_S(\mu_F^2)}{4\pi^2 b_0} \left[P_N^{(1)} - \frac{2\pi b_1}{b_0} P_N^{(0)} \right] \right\}. \end{aligned} \quad (18)$$

In Eq. (18), $D_{b,N}^{\text{ini}}(\mu_{0F}, m_b)$ is the N -space counterpart of Eq. (17); $P_N^{(0)}$ and $P_N^{(1)}$ are the Mellin transforms of the LO and NLO Altarelli–Parisi splitting functions, and their

expression can be found in [8]; b_0 and b_1 are the first two coefficients of the QCD β -function

$$b_0 = \frac{33 - 2n_f}{12\pi}, \quad b_1 = \frac{153 - 19n_f}{24\pi^2}, \quad (19)$$

which enter in the following expression for the strong coupling constant at a scale Q^2 :

$$\alpha_S(Q^2) = \frac{1}{b_0 \ln(Q^2/\Lambda^2)} \left\{ 1 - \frac{b_1 \ln[\ln(Q^2/\Lambda^2)]}{b_0^2 \ln(Q^2/\Lambda^2)} \right\}. \quad (20)$$

In (19), n_f is the number of active flavours. Equation (18) resums to all orders terms containing $\ln(\mu_F^2/\mu_{0F}^2)$. In particular, leading (LL) ($\alpha_S^n \ln^n(\mu_F^2/\mu_{0F}^2)$) and next-to-leading (NLL) ($\alpha_S^n \ln^{n-1}(\mu_F^2/\mu_{0F}^2)$) logarithms are resummed. For an evolution from $\mu_{0F} \simeq m_b$ to $\mu_F \simeq m_H$, mass logarithms $\ln(m_H^2/m_b^2)$ are hence resummed to NLL accuracy (collinear resummation). Moreover, setting $\mu_{0F} \simeq m_b$ in Eq. (17) prevents the logarithm $\ln(\mu_{0F}^2/m_b^2)$ from getting too large.

If the calculation were performed with a massive b quark, along the lines of Refs. [14, 15], contributions $\sim \alpha_S P_{qq}(x_b) \ln(m_H^2/m_b^2)$, equivalent to the collinear pole in massless approximation, would be found in the x_b differential spectrum. Hence, using the DGLAP evolution equations allows the large mass logarithms appearing in the massive computation to be resummed.

Before closing this section, I wish to point out that, for the purpose of factorization and collinear resummation, using in $D_b^{\text{ini}}(x_b, \mu_{0F}, m_b)$ and in the DGLAP evolution equations the pole or the $\overline{\text{MS}}$ b mass is not as essential as it is in the Yukawa coupling (7). In fact, both mass definitions lead to the same results within the given LL or NLL logarithmic accuracy. In the following, I shall assume that in Eq. (17) m_b is the pole mass and will let μ_{0F} run in the range $m_b/2 < \mu_{0F} < 2m_b$ in order to investigate the scale dependence of the prediction.⁴ The bottom pole mass has also been used in the phenomenological analyses of Refs. [11, 12, 17], within the framework of perturbative fragmentation functions.

4 Soft resummation

The $\overline{\text{MS}}$ coefficient function (10) and the initial condition of the perturbative fragmentation function (17) present terms $\sim 1/(1-x_b)_+$ and $\sim [\ln(1-x_b)/(1-x_b)]_+$ that become large once $x_b \rightarrow 1$, which corresponds to soft-gluon emission. In moment space, they correspond to single $\sim \ln N$ and double logarithms $\sim \ln^2 N$ for large values of the

⁴If one wanted to use the $\overline{\text{MS}}$ b mass $\bar{m}_b(\mu_m)$, μ_m should be taken of the order of m_b rather than m_H . In fact, according to the factorization formula (3), there is no dependence on m_H and on the hard-process variables in the perturbative fragmentation function $D_b(x_b, \mu_F, m_b)$.

Mellin variable N . Such contributions are process-independent in the initial condition of the perturbative fragmentation function, and have been resummed in [11] in the NLL approximation.

In this section I would like to present the results for soft resummation in the $\overline{\text{MS}}$ coefficient function. First, it is instructive to write Eq. (12) for large N :

$$\begin{aligned}\hat{\Gamma}_N(m_H, \mu, \mu_F) &= 1 + \frac{\alpha_S(\mu)C_F}{2\pi} \left[\ln^2 N + \left(\frac{3}{2} + 2\gamma - 2 \ln \frac{m_H^2}{\mu_F^2} \right) \ln N \right. \\ &\quad \left. + K(m_H, \mu_F) + \mathcal{O}\left(\frac{1}{N}\right) \right],\end{aligned}\quad (21)$$

where $K(m_H, \mu_F)$ contains terms that are constant with respect to N :

$$K(m_H, \mu_F) = \left(\frac{3}{2} - 2\gamma_E \right) \ln \frac{m_H^2}{\mu_F^2} + \frac{5}{6}\pi^2 + \frac{3}{2} + \frac{3}{2}\gamma_E + \gamma_E^2. \quad (22)$$

Furthermore, to get Eq. (21), I have used the large- N expansions of the polygamma functions:

$$\psi_0(N) \sim \ln N + \mathcal{O}\left(\frac{1}{N}\right), \quad (23)$$

$$\psi_1(N) \sim \mathcal{O}\left(\frac{1}{N}\right), \quad (24)$$

$$S_1(N) \sim \ln N + \gamma_E + \mathcal{O}\left(\frac{1}{N}\right), \quad (25)$$

$$S_2(N) \sim \frac{\pi^2}{6} + \mathcal{O}\left(\frac{1}{N}\right). \quad (26)$$

LL and NLL soft contributions to the $\overline{\text{MS}}$ coefficient function can be resummed following standard methods [18, 19].

In particular, all the steps that led to NLL resummation in the coefficient function for $e^+e^- \rightarrow q\bar{q}$ processes in Ref. [11] can be repeated, thus obtaining the resummed coefficient function for $H \rightarrow b\bar{b}$. In fact, in both processes one has in the final state two massless partons, as the b and \bar{b} are in the coefficient function, which are able to radiate soft- as well as collinear-enhanced radiation. The coefficients of $\ln N^2$ and $\ln N$ in Eq. (21) are indeed the same as in the large- N expansion of the e^+e^- coefficient function [11].

The resummed coefficient function can be obtained from the e^+e^- one, replacing the centre-of-mass energy squared Q^2 with m_H^2 . One obtains:

$$\ln \Delta_N = \int_0^1 dz \frac{z^{N-1} - 1}{1 - z} \left\{ \int_{\mu_F^2}^{m_H^2(1-z)} \frac{dk^2}{k^2} A[\alpha_S(k^2)] + \frac{1}{2} B[\alpha_S(m_H^2(1-z))] \right\}. \quad (27)$$

In Eq. (27), the two integration variables are $z = 1 - x_g$ and $k^2 = (p_b + p_g)^2(1 - z)$, as in [18]. In soft approximation, $z \simeq x_b$; for small-angle radiation, $k^2 \simeq k_T^2$, the gluon transverse momentum with respect to the b -quark direction.

The function $B(\alpha_S)$ is associated with the radiation emitted by the unobserved massless parton, namely the \bar{b} if one observes the b . The argument of $B(\alpha_S)$ is the invariant mass of the unobserved jet, i.e. $(p_{\bar{b}} + p_g)^2 \simeq m_H^2(1 - z)$ in soft approximation.

Moreover, Eq. (27) is formally equal to the resummed $\overline{\text{MS}}$ coefficient function in Drell–Yan and deep inelastic scattering (DIS) with light quarks [20]. For processes with massive quarks, such as top quark decay [17] or heavy quark production in DIS [21], recently provided with NLL soft resummation, the function $B(\alpha_S)/2$ should be replaced by a different one, called $S(\alpha_S)$ in Refs. [17] and [21], which is characteristic of processes with heavy quarks and expresses soft radiation, which is not collinear-enhanced. The function $A(\alpha_S)$ in Eq. (27) can be expanded as a series in α_S as:

$$A(\alpha_S) = \sum_{n=1}^{\infty} \left(\frac{\alpha_S}{\pi} \right)^n A^{(n)}. \quad (28)$$

The first two coefficients are mandatory to resum the coefficient function to NLL accuracy [18]:

$$A^{(1)} = C_F, \quad (29)$$

$$A^{(2)} = \frac{1}{2} C_F \left[C_A \left(\frac{67}{18} - \frac{\pi^2}{6} \right) - \frac{5}{9} n_f \right], \quad (30)$$

where $C_A = 3$. Likewise, the function $B(\alpha_S)$ can be expanded:

$$B(\alpha_S) = \sum_{n=1}^{\infty} \left(\frac{\alpha_S}{\pi} \right)^n B^{(n)} \quad (31)$$

and, to NLL level, only the first term of the expansion is kept:

$$B^{(1)} = -\frac{3}{2} C_F. \quad (32)$$

The integral over z can be performed making use of the replacement [18]:

$$z^{N-1} - 1 \rightarrow -\Theta \left(1 - \frac{e^{-\gamma_E}}{N} - z \right), \quad (33)$$

where Θ is the Heaviside step function. The function Δ_N can be expressed in the usual form:

$$\Delta_N(m_H, \mu, \mu_F) = \exp \left[\ln N g^{(1)}(\lambda) + g^{(2)}(\lambda, \mu, \mu_F) \right], \quad (34)$$

with

$$\lambda = b_0 \alpha_S(\mu) \ln N. \quad (35)$$

In Eq. (34) the term $\ln N g^{(1)}(\lambda)$ accounts for the resummation of the leading logarithms $\alpha_S^n \ln^{n+1} N$ in the Sudakov exponent, and the function $g^{(2)}(\lambda, \mu, \mu_F)$ resums NLL terms $\alpha_S^n \ln^n N$. Functions $g^{(1)}$ and $g^{(2)}$ can be obtained by simply setting $Q^2 = m_H^2$ in Eqs. (34) and (35) of Ref. [11]; the result is not here reported for the sake of brevity.

Following [11, 12, 21], I include in the Sudakov-resummed coefficient function the constant terms $K(m_H, \mu_F)$ defined in Eq. (22) and obtain:

$$\begin{aligned} \Delta_N^S(m_H, \mu, \mu_F) &= \left[1 + \frac{\alpha_S(\mu) C_F}{2\pi} K(m_H, \mu_F) \right] \\ &\times \exp \left[\ln N g^{(1)}(\lambda) + g^{(2)}(\lambda, \mu, \mu_F) \right]. \end{aligned} \quad (36)$$

Finally, the resummed result is matched to the fixed-order one, which will yield a prediction valid at $x_b < 1$ as well. The NLO result is added to Eq. (36) and, in order to avoid double counting, the $\mathcal{O}(\alpha_S)$ term of the resummed result is subtracted:

$$\begin{aligned} \hat{\Gamma}_N^{\text{res}}(m_H, \mu, \mu_F) &= \hat{\Gamma}_N^S(m_H, \mu, \mu_F) - \left[\hat{\Gamma}_N^S(m_H, \mu, \mu_F) \right]_{\alpha_S} \\ &+ \left[\hat{\Gamma}_N(m_H, \mu, \mu_F) \right]_{\alpha_S}, \end{aligned} \quad (37)$$

where $[\hat{\Gamma}_N^S]_{\alpha_S}$ and $[\hat{\Gamma}_N]_{\alpha_S}$ are respectively the expansion of Eq. (27) up to $\mathcal{O}(\alpha_S)$ and the full fixed-order coefficient function at $\mathcal{O}(\alpha_S)$ (12).

5 Bottom-quark energy distribution

In this section I present the energy spectrum of bottom quarks in Higgs decay, according to the calculation above described. I shall investigate the phenomenological effect of collinear and soft resummation, and the dependence of the prediction on factorization and renormalization scales. The results, which have been presented in analytic form in Mellin space, will be inverted numerically to x_b space choosing the integration contour according to the minimal prescription [22]. I shall plot the normalized rate $(1/\Gamma)(d\Gamma/dx_b)$, where Γ is the NLO $H \rightarrow b\bar{b}$ width, calculated in Refs. [14, 15]. I shall set $m_H = 120$ GeV, $m_b = 5$ GeV, $n_f = 5$, $\Lambda = 200$ MeV.

In Fig. 1 I have plotted the energy spectrum of the b -quark, according to the NLO massive calculation (dashed line), which can be obtained from Eq. (3) without evolving the perturbative fragmentation function, including collinear resummation (dotted line) and with both collinear and soft resummations (solid). I have set $\mu = \mu_F = m_H$, $\mu_0 = \mu_{0F} = m_b$.

We can notice a remarkable effect of both collinear and soft resummations. The fixed-order calculation lies below the resummed ones and grows as $x_b \rightarrow 1$ because of

a behaviour $\sim 1/(1 - x_b)$. The collinear-resummed spectrum exhibits instead a sharp peak at large x_b ; after both soft and collinear resummations, the distribution is further smoothed and presents the Sudakov peak at $x_b \simeq 0.97$.

Although one implements both collinear and soft resummations, the prediction is still not reliable at very small and large x_b . In fact, even the resummed distributions become negative once x_b approaches 0 or 1. At small x_b , the coefficient function contains a term $\sim \log x_b$ which has not been resummed yet; at very large x_b , one starts to get sensitive to missing non-perturbative power corrections. The range of reliability of a purely perturbative computation is typically $x_b \lesssim 1 - \Lambda/m_b$ [11].

In Figs. 2-5, I show the dependence of the prediction on the factorization and renormalization scales that appear in the calculation, i.e. μ and μ_F in Eq. (10), μ_0 and μ_{0F} in (17). I let μ and μ_F assume the values $m_H/2$, m_H and $2m_H$; as for the scales μ_0 and μ_{0F} , as discussed in Section 3, they will be taken equal to $m_b/2$, m_b and $2m_b$. The dependence on the scales is logarithmic, hence we expect it to be more visible once the scales vary around small values, i.e. around m_b rather than m_H .

Collinear resummation is turned on in all figures, but plots are with or without soft-gluon resummation. The general feature of these results is that after both collinear- and soft-enhanced terms are resummed, the final prediction exhibits very little scale dependence. In particular, we note that the role of soft resummation is crucial to weaken the dependence on scales μ_F (Fig. 2), μ_0 (Fig. 5) and especially μ_{0F} (Fig. 3). The dependence on the renormalization scale μ is instead very weak even resumming only collinear logarithms, as shown in Fig. 4. A milder sensitivity to renormalization and factorization scales corresponds to a reduction of the theoretical uncertainty on the result and is a meaningful effect of collinear and soft resummations.

Moreover, I would like to compare the b -quark energy distribution in three processes that have been investigated within the framework of perturbative fragmentation functions and provided with NLL collinear and soft resummations, namely $e^+e^- \rightarrow b\bar{b}$ [11], top decay $t \rightarrow bW$ [12,17] and, in this paper, Higgs decay. Because of the universality of the fragmentation process, possible differences in such spectra will be related to the different coefficient functions and mass scales involved. Furthermore, I shall consider e^+e^- at $\sqrt{s} = 91.2$ GeV, the centre-of-mass energy of LEP I and SLD, and, in order to test the effect of the coupling, vectorial in $e^+e^- \rightarrow b\bar{b}$ and scalar in $H \rightarrow b\bar{b}$, also at $\sqrt{s} = 120$ GeV, the default Higgs-mass value throughout this paper. In top decay I shall set $m_t = 175$ GeV and $m_W = 80$ GeV. From Fig. 6 one learns that the shapes of the three distributions exhibit some differences. The b spectrum in H decay is the highest at small x_b and the lowest at large x_b ; in top decay it is shifted toward large x_b and peaked very close to 1. The $e^+e^- \rightarrow b\bar{b}$ prediction lies within the other two at small and very large x_b . The effect of different values of \sqrt{s} in the e^+e^- process is visible mainly around the Sudakov peak; setting $\sqrt{s} = m_H$ makes the spectrum more similar

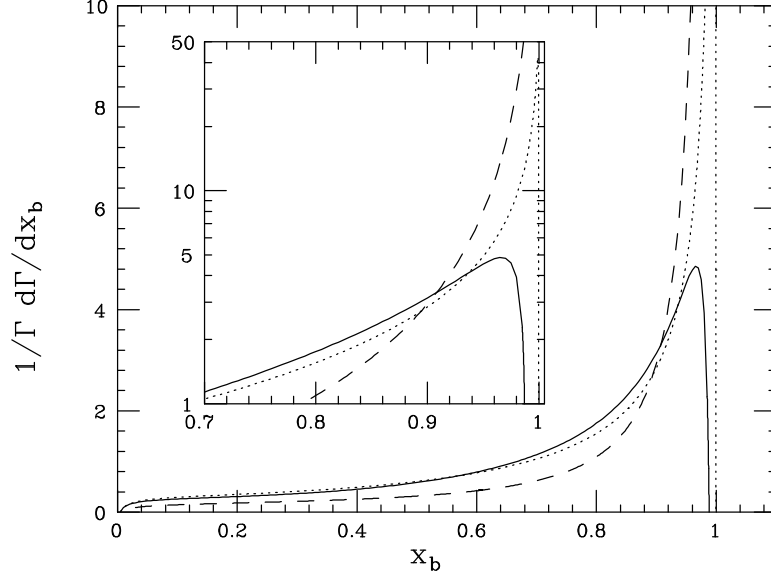


Figure 1: b -quark energy distribution in Higgs decay according to the NLO massive calculation (dashed line), including NLL collinear resummation (dots) and both NLL collinear and soft resummations (solid). I have set: $\mu = \mu_F = m_H$, $\mu_0 = \mu_{0F} = m_b$. In the inset figure, the same curves are shown at large x_b and on a logarithmic scale.

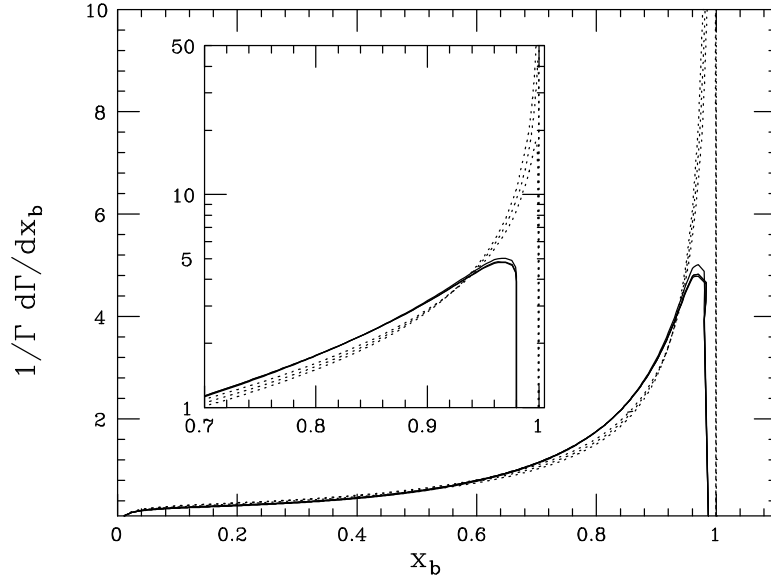


Figure 2: Dependence of the b spectrum on the factorization scale μ_F , with (solid lines) and without (dots) NLL soft resummation. The other scales are fixed at $\mu = m_H$ and $\mu_0 = \mu_{0F} = m_b$.

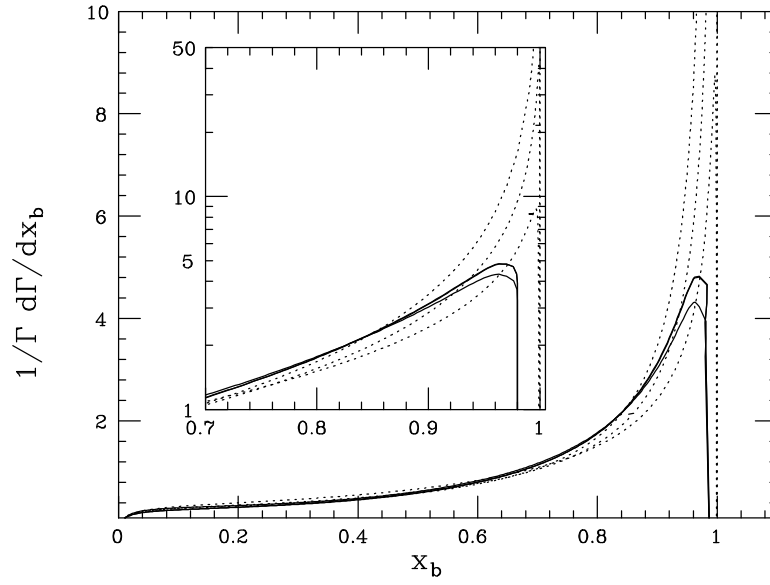


Figure 3: As in Fig. 2, but for different values of the factorization scale μ_{0F} . The other scales are fixed at $\mu = \mu_F = m_H$ and $\mu_0 = m_b$.

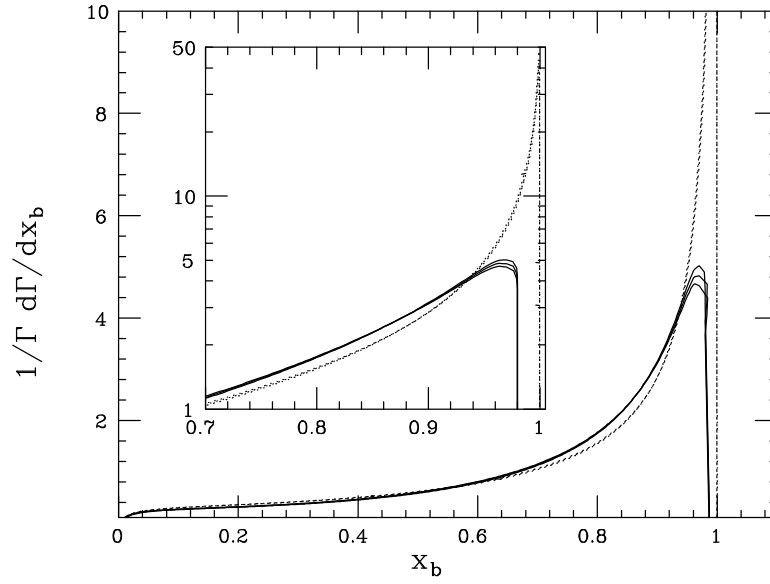


Figure 4: As in Fig. 2, but varying the renormalization scale μ . The other scales are fixed at $\mu_F = m_H$ and $\mu_{0F} = \mu_0 = m_b$.

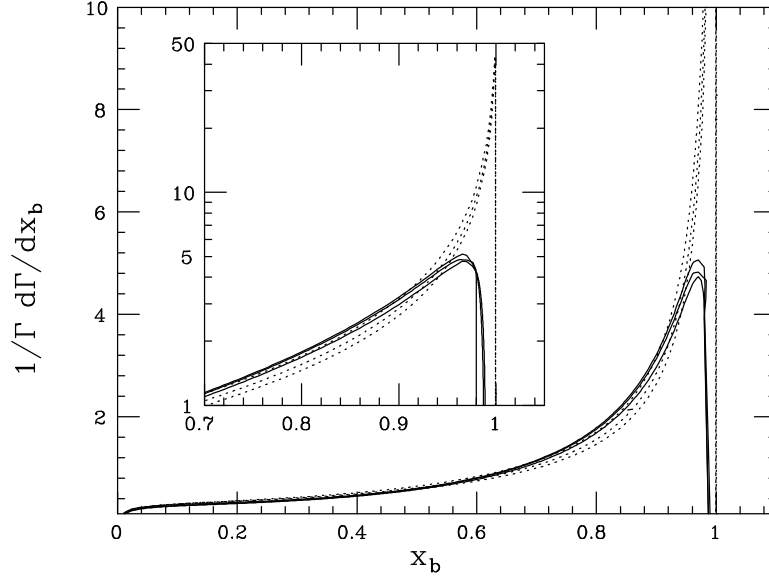


Figure 5: As in Fig. 4, but for different values of the renormalization scale μ_0 . The other scales are fixed at $\mu = \mu_F = m_H$ and $\mu_{0F} = m_b$.

to the Higgs decay one.

Before closing this section, it is interesting to investigate the dependence of the resummed prediction on the Higgs mass. In Fig. 7, we plot the NLL collinear- and soft-resummed spectrum for $m_H = 110, 120$ and 130 GeV. We note that the spectra change very little with the chosen value of m_H , and some small effect is only visible around the Sudakov peak.

6 Hadron-level results

I shall now present results on the energy spectrum of b -flavoured hadrons B in Higgs decay. Similarly to the parton-level analysis, for a hadron of momentum p_B one defines the B normalized energy fraction in the Higgs rest frame:

$$x_B = \frac{2p_B \cdot p_H}{m_H^2}. \quad (38)$$

Up to power corrections, one writes the hadron-level spectrum as the convolution of the parton-level one, calculated above, with the non-perturbative fragmentation function $D^{np}(x)$, associated with the hadronization of the b quark into the B hadron:

$$\frac{1}{\Gamma} \frac{d\Gamma_B}{dx_B}(x_B, m_H, m_b) = \frac{1}{\Gamma} \int_{x_B}^1 \frac{dz}{z} \frac{d\Gamma_b}{dz}(z, m_H, m_b) D^{np}\left(\frac{x_B}{z}\right). \quad (39)$$

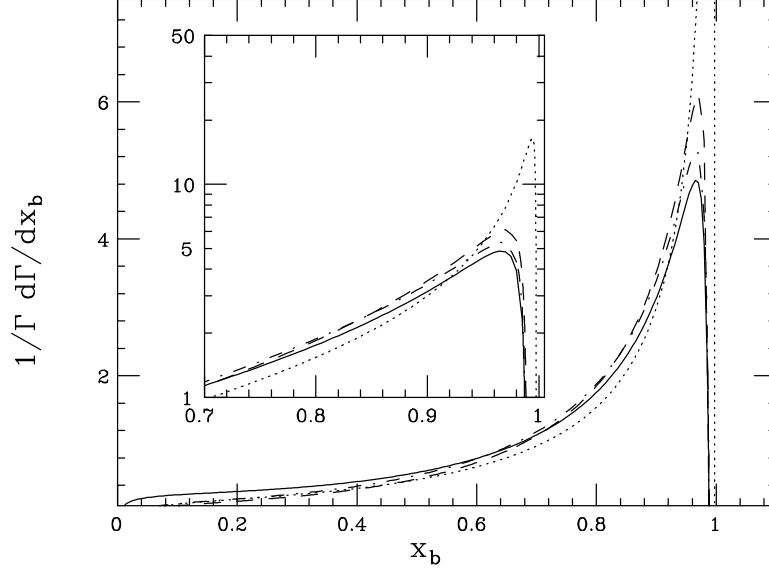


Figure 6: b -quark energy distribution in Higgs decay (solid), top decay (dots) and $e^+e^- \rightarrow b\bar{b}$ processes at $\sqrt{s} = 91.2$ GeV (dashes) and 120 GeV (dot-dashes). All predictions are given by a NLO calculation provided with NLL collinear and soft resummations. In Higgs decay I have set $\mu = \mu_F = m_H$, in top decay $\mu = \mu_F = m_t = 175$ GeV, in e^+e^- annihilation $\mu = \mu_F = \sqrt{s}$. All plots are for $\mu_0 = \mu_{0F} = m_b$.

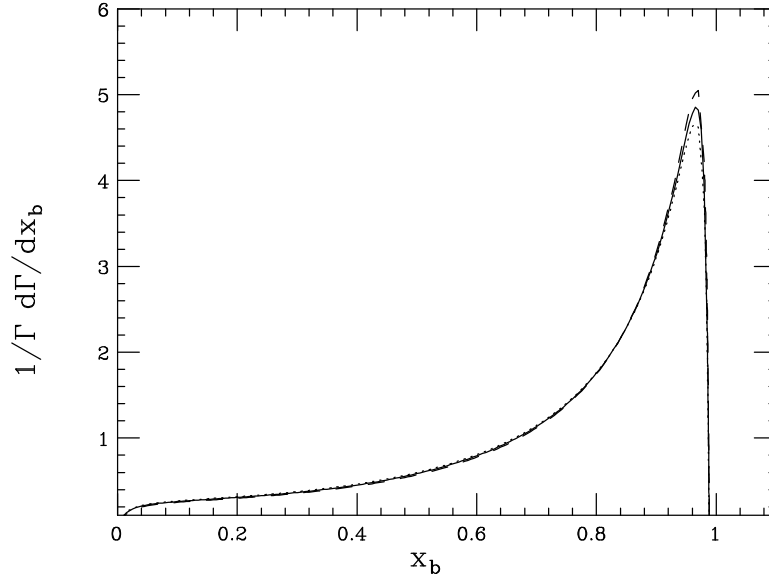


Figure 7: b -quark energy distribution in Higgs decay, including NLL collinear and soft resummations, for a Higgs mass of 110 GeV (dashes), 120 GeV (solid) and 130 GeV (dots).

The non-perturbative fragmentation function is to be extracted from experimental data. As the Higgs particle has not been discovered yet, one obviously does not have any data on B production in Higgs decay. However, relying on the universality of the hadronization transition, one can fit some hadronization models to data on B production in e^+e^- experiments and use them to predict the B spectrum in $H \rightarrow b\bar{b}$ processes. In order for the fitting procedure to be consistent, the $e^+e^- \rightarrow b\bar{b}$ perturbative process is to be described as done for Higgs decay. I shall have to use NLO coefficient functions, NLL collinear and soft resummation, and consistent values for the scales appearing in the calculation, e.g. $\mu = \sqrt{s}$ if I set $\mu = m_H$ in $H \rightarrow b\bar{b}$. In fact, it was recently found [23, 24] that such a consistency is crucial if one wishes to make use of non-perturbative information taken from e^+e^- data to describe the data on B -hadron production at hadron colliders, such as the Tevatron.

In this paper, as for the non-perturbative fragmentation function, I shall consider the following three hadronization models: a power law with two parameters

$$D^{np}(x; \alpha, \beta) = \frac{1}{B(\beta + 1, \alpha + 1)} (1 - x)^\alpha x^\beta, \quad (40)$$

the model of Kartvelishvili et al. [25]

$$D^{np}(x; \delta) = (1 + \delta)(2 + \delta)(1 - x)x^\delta \quad (41)$$

and the Peterson model [26]

$$D^{np}(x; \epsilon) = \frac{A}{x[1 - 1/x - \epsilon/(1 - x)]^2}. \quad (42)$$

In Eq. (40), $B(x, y)$ is the Euler beta function; in (42) A is a normalization constant. The parameters α , β , δ and ϵ are to be extracted from experimental data. In Ref. [17], such models have been fitted to ALEPH [27] data on B mesons and it was found that models (40) and (41) yield very good fits, while the Peterson model is marginally consistent. In Ref. [28], also the SLD data [29] were considered and it was found that Eqs. (40) and (41) lead to good fits, and Eq. (42) is instead unable to reproduce the SLD data. Moreover, using a soft-resummed perturbative calculation was essential to describe the SLD data. However, discrepancies were found in Ref. [28] between the best-fit parameters α , β and δ , according to whether one fits the models to ALEPH or SLD. Unlike ALEPH, the SLD data contain some b -flavoured baryons, mainly the Λ_b , but it is a pretty small fraction of the whole sample; hence, it may not be correct to conclude that the differences reported in [28] are due to the baryons reconstructed in SLD. Moreover, detailed analyses and comparisons on b -fragmentation in the four LEP experiments and SLD are currently missing.

Here I shall try instead a combined fit of both ALEPH and SLD data samples and investigate whether one is able to find a suitable parametrization of the hadronization

models (40)–(42) that would be consistent with both experiments. As in Refs. [12,17,28], I shall consider data for $0.18 \lesssim x_B \lesssim 0.94$, so as to avoid data points close to 0 or 1, where the presented calculation is not reliable. Furthermore, when doing the fits, I shall neglect the correlations among data points and sum statistical and systematic errors in quadrature.

α	0.90 ± 0.15
β	16.23 ± 1.37
$\chi^2(\alpha, \beta)/\text{dof}$	33.42/31
δ	17.07 ± 0.39
$\chi^2(\delta)/\text{dof}$	33.80/32
ϵ	$(1.71 \pm 0.09) \times 10^{-3}$
$\chi^2(\epsilon)/\text{dof}$	166.36/32

Table 1: Results of combined fits to $e^+e^- \rightarrow b\bar{b}$ data from ALEPH and SLD collaborations, using NLO coefficient functions, NLL DGLAP evolution and NLL soft-gluon resummation. I have set $\Lambda = 200$ MeV, $\mu_{0F} = \mu_0 = m_b = 5$ GeV and $\mu_F = \mu = \sqrt{s} = 91.2$ GeV. α and β are the parameters in the power law (40), δ refers to (41), ϵ to (42).

In Table 1 the best-fit parameters are quoted, along with the χ^2 per degree of freedom. Both power law and Kartvelishvili models fit the data quite well, while the Peterson non-perturbative model is unable to describe them. It is also interesting to investigate whether the implementation of soft resummation has an impact on the fit. Table 2 shows the best-fit parameters obtained without resumming soft-gluon contributions to the perturbative calculation of $e^+e^- \rightarrow b\bar{b}$. It should be noted that the fit gets worse and no hadronization model is capable of yielding a reasonably small χ^2/dof .

In Fig. 8 I present a prediction on the x_B distribution in Higgs decay, using the NLL collinear- and soft-resummed perturbative calculation, and the best-fit parameters of

α	1.01 ± 0.12
β	14.73 ± 0.94
$\chi^2(\alpha, \beta)/\text{dof}$	64.19/31
δ	14.67 ± 0.30
$\chi^2(\delta)/\text{dof}$	64.20/32
ϵ	$(2.76 \pm 0.14) \times 10^{-3}$
$\chi^2(\epsilon)/\text{dof}$	287.55/32

Table 2: As in Table 1, but without soft resummation in the parton-level calculation.

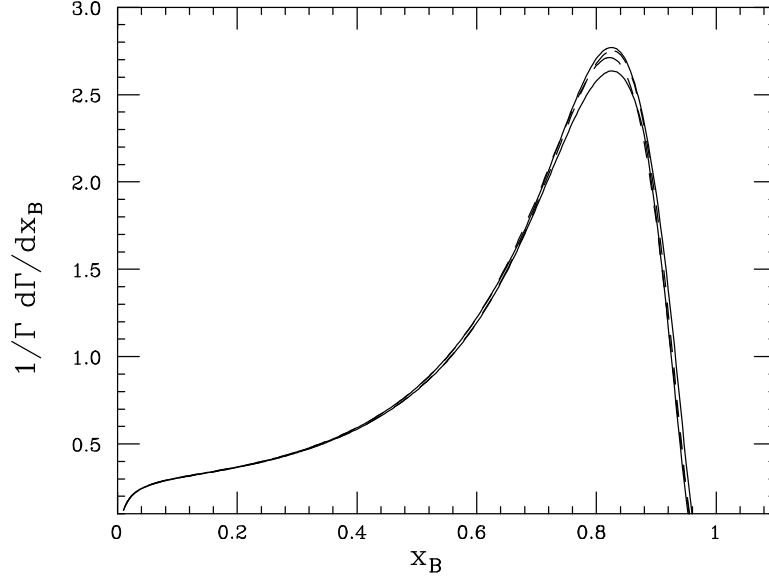


Figure 8: B -hadron spectrum in Higgs decay, modelling the hadronization according to the power law (40) (solid) and the Kartvelishvili model (41) (dashes). Plotted are the edges of bands at one-standard-deviation confidence level for the non-perturbative parameters α , β and δ , as reported in Table 1. In the perturbative calculation, the scales have been set to: $\mu = \mu_F = m_H = 120$ GeV, $\mu_0 = \mu_{0F} = m_b = 5$ GeV.

models (40) and (41) quoted in Table 1. I discard the Peterson model as it does not acceptably describe the considered data sample. In order to account for the errors on the best-fit parameters given in Table 1, for each model I plot a band corresponding to a prediction at one-standard-deviation confidence level for the fitted non-perturbative parameters α , β and δ .

Fig. 8 shows that the two predictions yielded by models (40) and (41) are statistically consistent. In fact, from Table 1 one learns that, within the error range, the parameter α of Eq. (40) is consistent with 1 and β of Eq. (40) is consistent with δ of Eq. (41). It is therefore reasonable that the predictions of the power law with two parameters and of the Kartvelishvili model agree.

As I did for the analysis at parton level, I present in Fig. 9 the B -hadron spectra in three different processes, i.e. e^+e^- annihilation, Higgs and top decay, using everywhere a NLO and NLL resummed perturbative calculation and the hadronization model (40), with the best-fit parameters reported in Table 1. As in the parton-level analysis, I make consistent choices for the scales involved and consider two centre-of-mass energies for the electron-positron process, i.e. $\sqrt{s} = 91.2$ and 120 GeV. For each process I plot a band corresponding to a prediction at one-standard-deviation confidence level for the parameters α and β of Eq. (40).

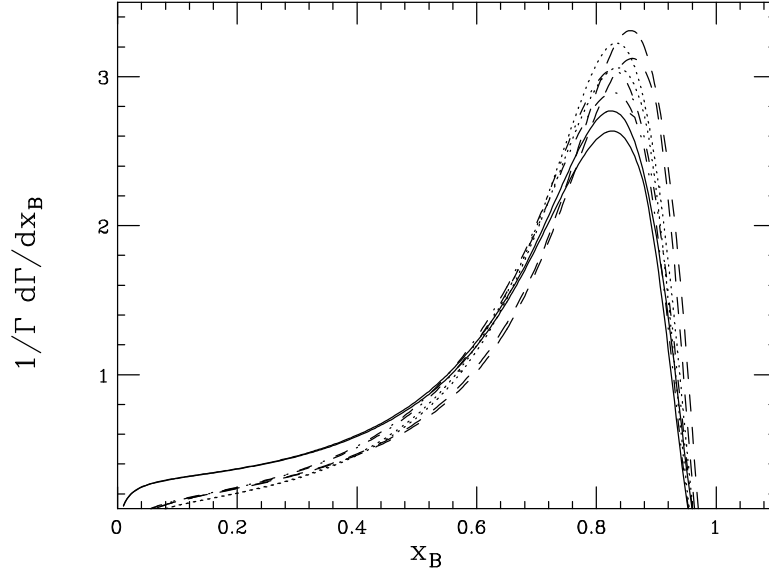


Figure 9: B -hadron spectra in Higgs decay (solid), in top decay (dashes) and in e^+e^- annihilation at $\sqrt{s} = 91.2$ GeV (dotted) and 120 GeV (dot-dashed), according to the hadronization model (40), at one-standard-deviation confidence level for the parameters α and β . Factorization and renormalization scales are chosen as in Fig. 6.

Figure 9 shows that the three spectra are statistically different and that the result is pretty similar to the one already found at parton-level in Fig. 6, which is reasonable as we are convoluting the x_b distribution with the same non-perturbative fragmentation function. Setting $\sqrt{s} = m_H$ makes the $e^+e^- \rightarrow b\bar{b}$ spectrum closer to the H -decay one, especially at middle and large values of x_B , though meaningful differences are still present at small x_B and around the peak.

Before closing this section, I would like to present results in moment space, using the experimental moments on B production in e^+e^- annihilation from the DELPHI Collaboration [30], along the lines of [17]. The advantage of working in moment space, as suggested in [23], is that one does not need to rely on any specific functional form of the non-perturbative fragmentation function. As done in [17], I have quoted in Table 3 the first four moments on B -production at DELPHI, the computed moments of e^+e^- and Higgs decay perturbative calculations, the extracted moments of the non-perturbative fragmentation function and the predictions for the moments of the B spectra in $H \rightarrow b\bar{b}$.

In moment space convolutions are turned into ordinary products, and we therefore have: $\sigma_N^B = \sigma_n^b D_N^{np}$, $\Gamma_N^B = \Gamma_N^b D_N^{np} = \Gamma_N^B \sigma_N^B / \sigma_N^b$, where σ_N and Γ_N are the moments of e^+e^- -annihilation cross section and Higgs-decay width at hadron or parton level. Comparing Table 3 with the results of [17], it should be noted that all considered moments in H decay are lower than those in e^+e^- processes and in top decay. This result is consistent with the spectra in x_B -space presented in Fig. 9.

	$\langle x \rangle$	$\langle x^2 \rangle$	$\langle x^3 \rangle$	$\langle x^4 \rangle$
e^+e^- data σ_N^B	0.7153 ± 0.0052	0.5401 ± 0.0064	0.4236 ± 0.0065	0.3406 ± 0.0064
e^+e^- NLL σ_N^b	0.7801	0.6436	0.5479	0.4755
D_N^{np}	0.9169	0.8392	0.7731	0.7163
H -decay NLL Γ_N^b	0.7578	0.6162	0.5193	0.4473
H -decay Γ_N^B	0.6948	0.5171	0.4015	0.3204

Table 3: Experimental data for the moments σ_N^B from DELPHI [30], the resummed e^+e^- perturbative calculations for σ_N^b [11], the extracted non-perturbative contribution D_N^{np} . Using the resummed perturbative result Γ_N^b , a prediction for the moments Γ_N^B in $H \rightarrow b\bar{b}$ processes is given. The experimental error should be propagated to the final prediction.

7 Conclusions

I have considered bottom-quark fragmentation in Standard Model Higgs decay $H \rightarrow b\bar{b}$ within the approach of perturbative fragmentation functions. I have computed the $\overline{\text{MS}}$ NLO coefficient function and resummed collinear logarithms $\ln(m_H^2/m_b^2)$ by using the DGLAP evolution equations in the NLL approximation. In the calculation of the coefficient function, the use of the $\overline{\text{MS}}$ -renormalized Yukawa coupling turned out to be essential.

I have resummed NLL soft terms in the coefficient function and matched the resummed result with the exact NLO one. Soft resummation in the coefficient function has been combined with the process-independent NLL soft resummation in the initial condition of the perturbative fragmentation function.

I have presented the b -quark energy spectrum in Higgs decay, which exhibits a remarkable effect of the implemented collinear and soft resummations. In particular, soft resummation smoothens the distribution at large x_b and the dependence of the prediction on factorization and renormalization scales turns out to be very little. The dependence of the predicted spectra on the Higgs mass is very small as well. I have also compared the b -energy spectrum in $H \rightarrow b\bar{b}$ with the ones yielded by top decay and $e^+e^- \rightarrow b\bar{b}$, which have been provided with NLL collinear and soft resummations in the framework of perturbative fragmentation.

I have then considered b -flavoured B -hadron production in Higgs decay in both x_B and moment space. I have fitted a few hadronization models to ALEPH and SLD data in x_B -space and used the best-fit parameters to predict the B spectrum in H decays. For this procedure to be consistent, the perturbative processes $e^+e^- \rightarrow b\bar{b}$ and $H \rightarrow b\bar{b}$ have been described using the same kind of calculation. The fits have shown that the power law with two tunable parameters and the Kartvelishvili model give good combined fits of ALEPH and SLD data, while the Peterson model is not capable of reproducing the

data. Moreover, implementing soft-gluon resummation in the coefficient function has been essential to be able to describe the data. The B -hadron spectra in Higgs decay according to the power law and to the Kartvelishvili model are in statistical agreement. The comparison of B spectra in $H \rightarrow b\bar{b}$, $t \rightarrow bW$ and $e^+e^- \rightarrow b\bar{b}$ exhibits similar features to the parton-level one. I have also made predictions for the first four moments of the B spectrum in $H \rightarrow b\bar{b}$ processes, using DELPHI data on the B moments in e^+e^- annihilation.

In conclusion, the presented calculation allows the performance of precise predictions for b -quark and B -hadron production in Higgs decay and could be applied for analyses of Higgs phenomenology at the Tevatron and ultimately at the LHC. The computed NLO matrix elements, along with NLL DGLAP evolution and soft resummation, can be used for further investigations of other observables in Higgs decay. In particular, studies of the transverse momentum distributions of b quarks and b -flavoured hadrons are under way. Moreover, as the NNLO initial condition of the perturbative fragmentation function has recently been computed [16], the coefficient function may be calculated to NNLO as well and a resummation of collinear and soft terms to next-to-next-to-leading logarithmic accuracy can be made.

Acknowledgements

I am grateful to M. Cacciari, who provided me with the computer code to perform inverse Mellin transforms and fits of hadronization models to e^+e^- data. I thank S. Catani, L. Magnea, F. Maltoni, S. Moretti and M.H. Seymour for several discussions on these and related topics. I acknowledge V. Ravindran for pointing out an error in Eq. (10) in the first version of the paper.

References

- [1] K.A. Assamagan et al. [Higgs Working Group], hep-ph/0406152.
- [2] ALEPH, DELPHI, L3, OPAL, The LEP Working Group for Higgs Boson Searches, Phys. Lett. B565 (2003) 61.
- [3] L. Babukhadia et al. [CDF and D0 Working Group Members Collaboration], FERMILAB-PUB-03-320-E.
- [4] ATLAS TDR on Physics performance, Vol. II, Chap. 19, *Higgs Bosons* (1999); CMS TP, CERN/LHC 94-38 (1994).

- [5] V. Drollinger, Th. Müller and D. Denegri, CMS Note 2001/054, hep-ph/0111312.
- [6] V. Drollinger, Th. Müller and D. Denegri, CMS Note 2002/006, hep-ph/0201249.
- [7] M.L. Mangano, M. Moretti, F. Piccinini, R. Pittau and A.D. Polosa, Phys. Lett. B556 (2003) 50.
- [8] B. Mele and P. Nason, Nucl. Phys. B361 (1991) 626.
- [9] G. Altarelli and G. Parisi, Nucl. Phys. B126 (1977) 298.
- [10] L.N. Lipatov, Sov. J. Nucl. Phys. 20 (1975) 95; V.N. Gribov and L.N. Lipatov, Sov. J. Nucl. Phys. 15 (1972) 438; Yu.L. Dokshitzer, Sov. Phys. 46 (1977) 641.
- [11] M. Cacciari and S. Catani, Nucl. Phys. B617 (2001) 253.
- [12] G. Corcella and A.D. Mitov, Nucl. Phys. B623 (2002) 247.
- [13] J. Campbell, R.K. Ellis, F. Maltoni and S. Willenbrock, Phys. Rev. D67 (2002) 095002.
- [14] E. Braaten and J.P. Leveille, Phys. Rev. D22 (1980) 715.
- [15] M. Drees and K. Hikasa, Phys. Lett. B240 (1990) 455, Erratum-ibid. B262 (1991) 497.
- [16] K. Melnikov and A.D. Mitov, Phys. Rev. D70 (2004) 034027.
- [17] M. Cacciari, G. Corcella and A.D. Mitov, JHEP 0212 (2002) 015.
- [18] S. Catani and L. Trentadue, Nucl. Phys. B327 (1989) 323.
- [19] G. Sterman, Nucl. Phys. B281 (1987) 310.
- [20] S. Catani, G. Marchesini and B.R. Webber, Nucl. Phys. B349 (1991) 635.
- [21] G. Corcella and A.D. Mitov, Nucl. Phys. B676 (2004) 346.
- [22] S. Catani, M.L. Mangano, P. Nason and L. Trentadue, Nucl. Phys. B478 (1996) 273.
- [23] M. Cacciari and P. Nason, Phys. Rev. Lett. 89 (2002) 122003.
- [24] M. Cacciari, S. Frixione, M.L. Mangano, P. Nason and G. Ridolfi, JHEP 0407 (2004) 033.
- [25] V.G. Kartvelishvili, A.K. Likhoded and V.A. Petrov, Phys. Lett. B78 (1978) 615.

- [26] C. Peterson, D. Schlatter, I. Schmitt and P.M. Zerwas, Phys. Rev. D27 (1983) 105.
- [27] ALEPH Collaboration, A. Heister et al., Phys. Lett. B512 (2001) 30.
- [28] G. Corcella, hep-ph/0409120.
- [29] SLD Collaboration, K. Abe et al., Phys. Rev Lett. 84 (2000) 4300.
- [30] DELPHI Collaboration, ICHEP 2002 Note, DELPHI 2002-069 CONF 603.